EXPERIMENTAL STUDIES ON THE STRUCTURE OF PULVERIZED COAL FLAMES

A Pinto and S. R. Gollahalli

School of Aerospace, Mechanical, and Nuclear Engineering, The University of Oklahoma, Norman, Oklahoma 73019

The effects of varying primary air flow rate, secondary air flow rate, and coal feeding rate on the structure of pulverized bituminous coal flames have been studied experimentally. The changes in flame appearance, flame length, axial and radial temperature profiles, and volumetric concentration of particulate matter have been measured by means of color photography, thermocouples and He-Ne laser beam attenuation. Combustion in the near-nozzle region is seen to be diffusion-controlled, whereas heat release in the far-nozzle region is seen to be governed by the heterogeneous oxidation processes.

INTRODUCTION

Estimates and projections of the availability of various energy resources have indicated that even by the end of the present century, when nuclear, solar, and geothermal energies are expected to play a prominent role, fossil fuel combustion should still contribute about 80 percent of the energy used in the United States (1). It is widely recognized that coal will play an increasingly important role as an energy source worldwide and particularly in the United States because of her large coal reserves. Although the recent efforts to develop methods of coal gasification, coal liquefaction, and fluidized-bed combustion appear to be promising, at present their technology is still in its infancy. Hence, at present and in the near future coal used for generation of electricity will be in the pulverized form. Therefore, to provide a short-term solution to the energy problem, it is necessary to devise more efficient and environmentally acceptable methods of burning pulverized coal of different ranks. Some problems that are currently plaguing pulverized coal combustion are (i) necessity of using a large excess of air, which requires considerable amounts of energy to pump and produces much SO_x and NO_x (2), (ii) stability problems that arise with changes in coal properties when coals of different types are used, and (iii) emission of particulates. To devise solutions to these problems, it is essential to understand the structure and dominant physicochemical processes of pulverized coal flames. Although several studies on large full-scale industrial-size burners can be found in the literature (3, 4, 5, 6), diagnostic experimental investigations, particularly on the flame structure and its effect on gaseous pollutant formation in pulverized coal flames, are largely lacking. Hence, this paper presents the results of the first phase of a detailed experimental investigation being carried out at the University of Oklahoma, which is directed to provide comprehensive information on the effects of operating and fuel variables on the structure of pulverized coal flames.

MATERIALS AND METHODS

Figure 1 shows the schematic diagram of the experimental apparatus used for this study. It consisted of a stainless steel cylindrical combustion chamber mounted horizontally on an asbestos-topped table. The chamber had four windows, each 27 cm long and 4 cm wide, mounted two on each side. Primary air that carried the pulverized coal to the combustion chamber was supplied from the laboratory compressed air line through suitable regulators and flow meters. Pulverized coal stored in a hopper was supplied to the primary air line by means of a helical lead screw which was coupled to a variable-speed electric motor. A divergent nozzle was attached to the end of the primary air/coal-carrying tube in order to increase the stability range of the flame. Secondary air required for combustion was supplied by means of a variable-speed air blower through a settling chamber and several holes drilled in the plate mounted on the upstream end of the combustion chamber. The filter medium contained in the settling chamber served to provide a uniform velocity profile of secondary air flow at the entrance to the combustion chamber. A pilot burner fueled with propane gas was mounted near

the coal nozzle. Exhaust from the combustion chamber was led to atmosphere through suitable baffles in order to prevent back flow of outside air.

Coal feeding rate was measured by noting the rotational speed of the feeding screw and using a calibration graph of $\dot{m}_c$ vs speed prepared earlier. Air and propane gas flow rates were measured by means of flowmeters. Flames were photographed in color to document the changes in appearance and flame length with changes in the operating variables. The temperature field was probed by means of a chromel-alumel thermocouple and the readings were corrected for radiation and conduction losses by the method of King and Lynn (7). The total radiation emittance of the flame normal to the axis was determined with a water-cooled heat flux meter. The attenuation of a 4-mW He-Ne gas laser beam while passing through the flame normal to its axis was recorded by means of a laser power meter and the volumetric concentration of particulates was estimated. Bituminous coal pulverized so that 60.8% of it passed through a 200-mesh screen (76 μm) was used in this study. The details of the experimental facility and the instrumentation can be found in a thesis (8).

RESULTS

Flame Appearance and Length

In the absence of coal powder in the primary air, the opposed jet flame formed by the pilot gas burner was highly turbulent, with a yellowish periphery and bluish core. As the coal feed rate was increased, the flame color changed from blue to yellow in the core region while the yellow color at the periphery remained the same. The visible flame length (1) increased with the increase in coal feed rate ($\dot{m}_c$) (Figure 2). At the largest coal feed rate used in this study, the flame was very turbulent and exhibited a tendency to curve upwards at the tip.

Figure 3 shows the effects of increasing primary air flow rate ($\dot{m}_{pa}$) on flame length at two levels of coal feeding rate ($\dot{m}_c$), while other parameters were kept invariant. At low values of $\dot{m}_{pa}$ the flames became brighter, more luminous and longer. Flame length attained a peak value at certain $\dot{m}_{pa}$ and then decreased with further increase in $\dot{m}_{pa}$.

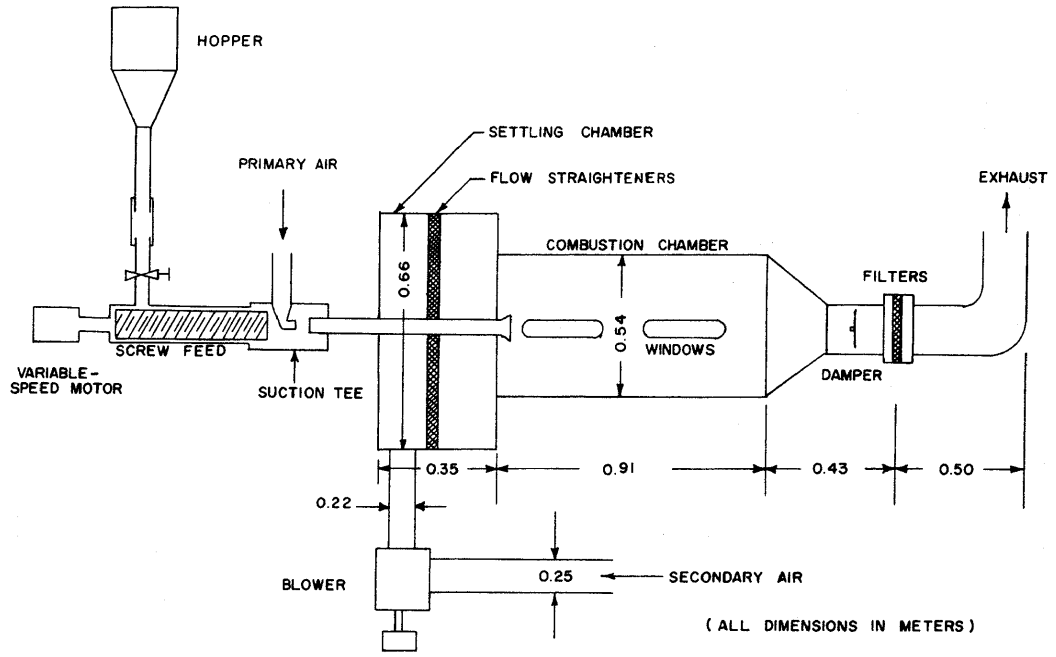

FIGURE 1. Schematic diagram of the experimental setup.

Flame length was seen to be significantly decreased when the secondary air flow rate ($\dot{m}_{sa}$) was increased (Figure 4). At low values of $\dot{m}_{sa}$ the color was bright yellow uniformly all over the flame. With increase in $\dot{m}_{sa}$, the flame turned bluish near the periphery and remained yellow in the core region.

Temperature Profiles

The variation of temperature along the axis of four typical flames is shown in Figure 5. Curve A is the axial temperature profile in the flame at a set of base conditions and curves B, C, and D are axial temperature profiles in flames in which $\dot{m}_c$, $\dot{m}_{pa}$, and $\dot{m}_{sa}$ respectively were changed from the base conditions. A comparison of curves A and B reveals that an increase in coal feed rate decreased the temperature near the nozzle and caused a peak in the temperature profile. Similar effect would occur if $\dot{m}_{pa}$ were decreased (curves A and C). On the other hand, an increase in $\dot{m}_{sa}$ not only decreased axial temperature in the near-nozzle region but also caused a more rapid decline of temperature profile downstream.

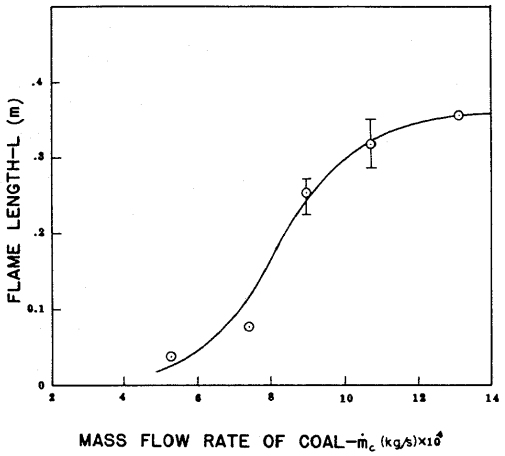

FIGURE 2. Variation of flame length with coal feed rate ($\dot{m}_{pa}$ = 0.0018 kg/s, $\dot{m}_{sa}$ = 0.072 kg/s, $\dot{m}_g$ = 1.72 × 10^{-7} kg/s).

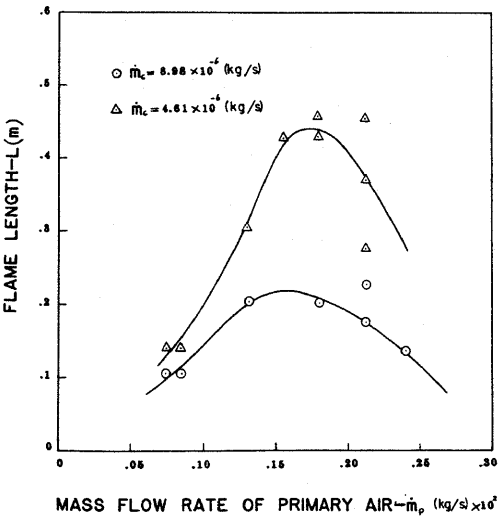

FIGURE 3. Effect of primary air flow rate on flame length ($\dot{m}_{sa}$ = 0.072 kg/s, $\dot{m}_g$ = 1.72 × 10^{-7} kg/s).

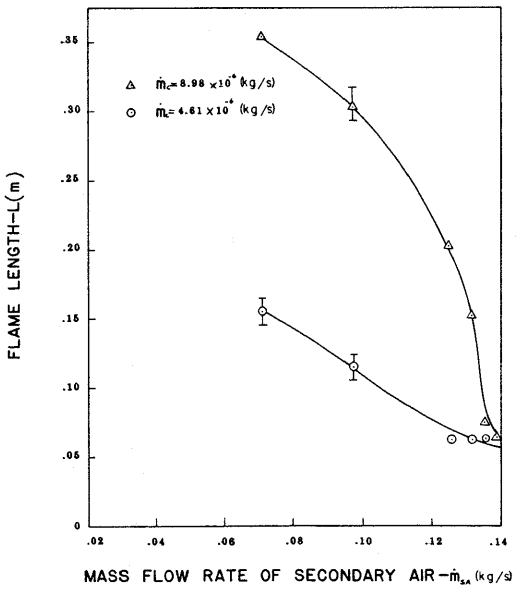

FIGURE 4. Effect of secondary air flow rate on flame length ($\dot{m}_{pa}$ = 0.0018 kg/s, $\dot{m}_g$ = 1.72 × 10^{-7} kg/s.

Figure 6 shows the effects of varying $\dot{m}_c$, $\dot{m}_{pa}$, and $\dot{m}_{sa}$ on radial temperature profiles in the near-nozzle region. In the near-nozzle region, either increasing $\dot{m}_c$ (curve B) or decreasing $\dot{m}_{sa}$ (curve C) from the base conditions (curve A) showed the same effect of flattening the radial temperature profile, whereas increasing $\dot{m}_{sa}$ (curve D) caused a more rapid decrease in temperature radially outwards. Also, in the same figure, the radial temperature profile in the far-nozzle region of the flame at the base conditions is shown (curve E), which indicates that a sharper decline of temperature would occur in the radially outward direction in the far-nozzle region than in the near-nozzle region.

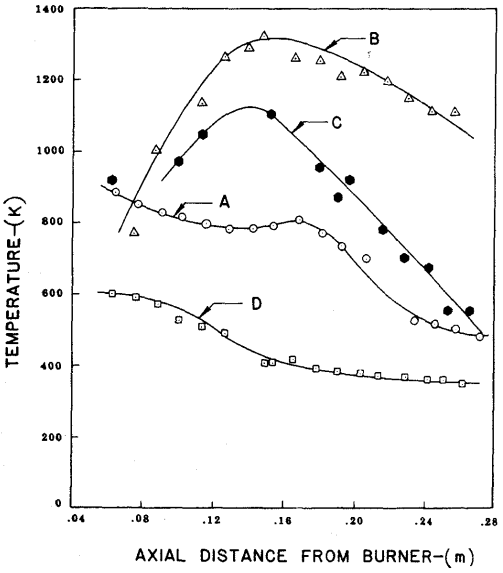

FIGURE 5. Effects of primary air flow rate, secondary air flow rate, and coal feed rate on axial temperature profiles.
CURVE A: $\dot{m}_c = 4.44 \times 10^{-4}$ kg/s, $\dot{m}_{pa} = 0.0018$ kg/s, $\dot{m}_{sa} = 0.072$ kg/s, $\dot{m}_g = 1.72 \times 10^{-7}$ kg/s.
CURVE B: $\dot{m}_c = 8.98 \times 10^{-4}$ kg/s, $\dot{m}_{pa} = 0.0018$ kg/s, $\dot{m}_{sa} = 0.072$ kg/s, $\dot{m}_g = 1.72 \times 10^{-7}$ kg/s.
CURVE C: $\dot{m}_c = 4.44 \times 10^{-4}$ kg/s, $\dot{m}_{pa} = 0.0014$ kg/s, $\dot{m}_{sa} = 0.072$ kg/s, $\dot{m}_g = 1.72 \times 10^{-7}$ kg/s.
CURVE D: $\dot{m}_c = 4.44 \times 10^{-4}$ kg/s, $\dot{m}_{pa} = 0.0018$ kg/s, $\dot{m}_{sa} = 0.132$ kg/s, $\dot{m}_g = 1.72 \times 10^{-7}$ kg/s.

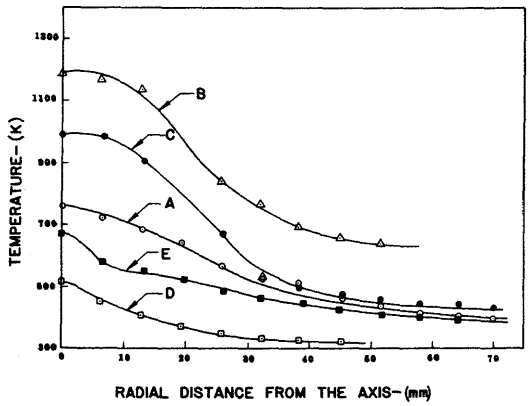

FIGURE 6. Effects of primary air flow rate, secondary air flow rate, and coal feed rate on radial temperature profiles. Operating conditions of curves A, B, C, and D were the same as those of corresponding curves on Figure 5 and axial distance x at which radial profiles were taken is equal to 0.25 flame length from the nozzle; operating conditions of curve E were the same as those of curve A, but the axial distance was 0.75 flame length from the nozzle.

Particulate Concentration

The variation of the ratio of volumetric concentration of particulates (W) to that near the burner (W_o), estimated from the measured laser beam attenuation readings by the method of Yagi and Iino (9), along the axis of the flame at the base conditions is shown in Figure 7. Although there is a large scatter in the results, caused by the uncertainties in the estimation of instantaneous path length of absorption, the tendency of W to increase along the axis is clear.

DISCUSSION

The changes in the flame appearance and the quantitative results given above clearly show that the structure of the pulverized coal flame is very sensitive to the coal feeding rate, primary air flow rate, and secondary air flow rate.

The blue region in the core of the pilot gas flame is caused by the highly turbulent mixing between the gas and primary air and gas-phase oxidation reactions are dominant in that region. As the coal feed rate

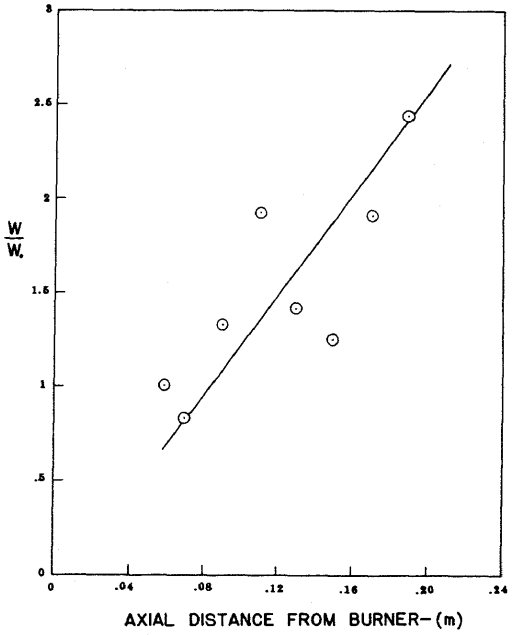

FIGURE 7. Variation of volumetric concentration of particulates along the axis ($\dot{m}_{pa} = 0.0018$ kg/s, $\dot{m}_{sa} = 0.072$ kg/s, $\dot{m}_c = 4.44 \times 10^{-4}$ kg/s, $\dot{m}_g = 1.72 \times 10^{-7}$ kg/s, W = local particulate concentration, W_o = particulate concentration at the nozzle.)

is increased, the flame turns yellow because of the continuous radiation emitted by the solid particles. The axial temperature in the near-nozzle region decreases with the increase in $\dot{m}_c$ for two reasons. First, the sensible heat required to raise the solid particles to their pyrolysis temperature is absorbed. Second, the pyrolysis reactions resulting in devolatilization are endothermic. The release and subsequent diffusion-controlled combustion of volatile products of pyrolysis are manifested in the broadening of the radial temperature profiles near the axis. Although sharp off-axis peaks characteristic of pure laminar gas diffusion flames are not seen because of the presence of primary air, the extension of the heat-release zone radially outward indicates that diffusion-controlled heat release is as important as the kinetics-controlled combustion in the near-nozzle region of pulverized coal flames. The flame is also elongated with the increase in $\dot{m}_c$, because of (i) slower heterogeneous reactions of coal char in the downstream region of the nozzle and (ii) increased mass flow rate of fuel to be burnt. The flame length vs m curve eventually levels off when all air that can be entrained at that particular set of operating conditions is consumed.

A conspicuous difference exists between the structure of the flames in the present study, where a small amount of gaseous fuel (although less than 0.1% of the mass flow rate of coal) was fed to the near-nozzle region, and that in the large-scale flames studied in References 3, 4, and 5. In the flames described by these References ignition of coal particles occurred always at a certain distance (which is called "ignition distance" in those studies) away from the burner nozzle, whereas in the present study the flames always started right near the nozzle. Ignition distance was seen to be considerably affected when operating parameters were changed in those studies. Since combustion in gas flames in the downstream parts of the flame is seen to be markedly affected by the magnitude of the ignition distance and the entrainment of air in that region (10), it is possible that those variables which change ignition distance in pulverized fuel flames also will change the combustion in the subsequent zones. As ignition distance in the present experiment was almost zero and was invariant with $\dot{m}_c$, $\dot{m}_{pa}$, and $\dot{m}_{sa}$, the influence of these variables on flame stability is minimal in the present arrangement as compared to that in flames of References 3-5.

The effects of primary air flow rate can be attributed to the changes in availability of oxygen and residence time of coal particles in the flame region. As $\dot{m}_{pa}$ is increased, the velocity in the axial direction increases and the residence period of coal particles decreases and thus leads to lengthening of visible flames. On the other hand, increased availability of oxygen accompanying the increase in $\dot{m}_{pa}$ increases the reaction rate and thus leads to shortening of the flames. The combined effects of these two factors are responsible for the peaking of the flame length vs primary air flow rate curve. At low values of $\dot{m}_{pa}$, the insufficiency of available oxygen in the near-nozzle region also causes the occurrence of maximum axial temperature away from the burner nozzle. Flattening of radial temperature profiles when $\dot{m}_{pa}$ was decreased is also caused by the decrease in the oxygen supply in the core, which leads to significant proportions of diffusion-controlled combustion with ambient air.

When secondary air flow rate is increased, the mixing between primary air/coal jet and the secondary air is enhanced and increased entrainment of air occurs. This results in higher rates of oxidation reactions in both homogeneous and heterogeneous processes and leads to a reduction of flame length and increase in luminosity. The increased momentum of the flame jet also counteracts the effects of buoyancy and confines the flame to the axial region. Lower peak temperatures noticed in flames with higher $\dot{m}_{sa}$ are probably caused by the more rapid dilution of the flame. The variation of flame length with $\dot{m}_{sa}$ is contrary to that noticed by Loisson and Kissel (5) in their experiments on large flames, primarily because of the difference in the ignition distance and its change with $\dot{m}_{sa}$ between the present study and that of Loisson and Kissel. The more rapid decline of temperature profiles in the radially outward direction further suggests that the extent of diffusion-controlled combustion of volatile decreases at higher $\dot{m}_{sa}$.

In the near-nozzle region coal particles are suspended in the primary air stream. As they proceed along the flame, they lose

their volatiles content and because of their relatively larger momentum are confined to the axial region. Because of the closely grouped confinement of char particles in the downstream parts of the flame, their volumetric concentration increases with the axial distance.

A comparison of the flame length data at some typical conditions with the flame lengths predicted by the theoretical formulations of Sunavala (11) and Bhaduri and Bandopadhyay (12) shows that the predictions of the latter agree well with measured values, whereas the predictions of the former exceed experimental values by a factor of three.

CONCLUSIONS

This study has shown that the structure of pulverized coal flames is strongly dependent on coal feed rate, primary air flow rate, secondary air flow rate, and introduction of additional gaseous fuel into the near-nozzle region. Combustion in the near-nozzle region is seen to be diffusion-controlled, whereas in the downstream region heterogeneous reaction processes are seen to dominate. An increase of coal feed rate increases flame length and shifts the location of peak flame temperatures downstream. An increase in secondary air flow rate decreases flame length and maximum temperature whereas the effects of increasing primary air flow rate on flame characteristics depend upon its magnitude. Injection of small amounts of additional gaseous fuel into the near-nozzle region enhances the stability of the pulverized coal flame and reduces the sensitivity of flame characteristics to the changes in operating variables.

REFERENCES

1. A. K. OPPENHEIM and F. J. WEINBERG, Astronaut. Aeronaut.: 22-31 (1974).
2. J. O. L. WENDT, C. V. STERNLING, and M. A. MATOVICH, Fourteenth Symposium (International) on Combustion, The Combustion Institute, Pittsburgh, Pa., 1973, pp. 897-904.
3. J. M. BEER, J. Inst. Fuel 36: 386-413 (1963).
4. J. M. BEER and N. A. CHIGIER, J. Inst. Fuel 42: 443-450 (1969).
5. R. LOISSON and R. R. KISSEL, J. Inst. Fuel 35: 60-73 (1962).
6. E. H. HUBBARD, J. Inst. Fuel 33: 386-399 (1960).
7. W. J. KING and W. LYNN, Trans. Am. Soc. Mech. Engrs. 65: 421-423 (1943).
8. A. PINTO, *Combustion of Pulverized Coal*, M.S. Thesis, University of Oklahoma, Norman, Oklahoma, 1978.
9. S. YAGI and H. IINO, Eighth Symposium (International) on Combustion, The Combustion Institute, Pittsburgh, Pa., 1962, pp. 288-293.
10. S. R. GOLLAHALLI , Can. J. Chem. Eng. 56: 510-514 (1978).
11. P. D. SUNAVALA, J. Inst. Fuel 41: 477-483 (1968).
12. D. BHADURI and S. BANDYOPADHYAY, Combustion Flame 17: 15-24 (1971).